KSCE Journal of Civil Engineering (2010) 14(5):699-707
DOI 10.1007/s12205-010-0838-5

Geotechnical Engineering
www.springer.com/12205

Effect of a Front High Hydraulic Conductivity Zone on Hydrological Behavior of Subsea Tunnels

Eun-Soo Hong*, Eui-Seob Park, Hee-Soon Shin***, and Hyung-Mok Kim******

Received April 12, 2009/Revised November 18, 2009/Accepted February 2, 2010

Abstract

This study focuses on the hydrological behavior of the ground ahead of a tunnel face. A localized high hydraulic conductivity zone with high water pressure is denoted as a hazardous zone. To analyze the impact of the hazardous zone on the face stability, a new indicator (TSR: the ratio of the driving force to the resisting force) is proposed on the basis of the "advance core" concept (Lunardi, 2000). A series of three-dimensional steady-state seepage analyses are performed to estimate the distribution of the TSR of the ground ahead of the tunnel face. The analyses results show that the hydrostatic pore water pressure acts on the most of the hazardous zones throughout all of the tunnelling stages. When the distance between the tunnel face and the hazardous zone (d_h) value is approximately five times the excavated tunnel radius, the influence of the hazardous zone increases rapidly.

Keywords: *face stability, hazardous zone, hydraulic gradient, subsea tunnel, water pressure*

1. Introduction

Tunneling under a water table induces geotechnical problems that include reductions in the face stability and tunneling performance due to the presence of groundwater. Especially in subsea tunneling, these problems are aggravated by localized site investigations and unforeseen geological conditions. Most subsea tunnel routes are located under poor environmental conditions that are characterized by such factors as major fault zones and high water pressure. Hong *et al*. (2007) analyzed the causes of several tunnel flooding cases and found that the presence of unforeseen high hydraulic conductivity zones with high water pressure (herein, termed as hazardous zones) was strongly associated with various flooding accidents. The localized high-hydraulic conductivity zones are considered "fault breccia" (Buergi *et al*., 1999; Sausgruber and Brandner, 2003; Wise *et al*., 1984) that consist of cohesionless materials and that show high hydraulic conductivity and porosity. High water pressure in a fault breccia zone can lead to significant problems related to the stability of the tunnel face. If the fault breccia zone has an infinite source of inflow water (e.g., from an aquifer or as seawater), a flooding accident will occur at the tunnel face. Thus, it is important to study the effect of hazardous zones on the hydraulic behavior of subsea tunnels.

Many researchers, such as Leca and Panet (1988), Leca and Dormineux (1990), El Tani (2003), Schweiger *et al*. (1991), Bobet (2001), Lee and Nam (2001), Kong *et al*. (2006), Park *et al*. (2008), and Arjnoi *et al*. (2009) have studied the effect of water pressure and/or the seepage force on the stability of tunnels driven under the water table. Schubert and Steindorfer (1998), Jeon *et al*. (2005), and Baek *et al*. (2006) carried out studies of the stability and behavior of tunnels with localized fracture zones such as faults. However, few studies exist regarding the effects of high water pressure on the stability of a tunnel face affected by a fracture zone ahead of the tunnel.

The failure mechanisms of tunnel faces have been studied by a number of researchers (Leca and Pannet, 1988; Leca and Dormineux, 1990; Anagnostou and Kovari, 1996, among others). These studies have mainly concentrated on shallow tunnels. In a large and deep tunnel, face stability is more significant owing to the plastic extrusion of the tunnel face (Hoek, 2001). Recently, Lunardi (2000) suggested the advance core concept. An advance core is a cylindrically shaped volume of ground ahead of the face; the radius of the cylinder is approximately equal to the radius of the tunnel. As shown in Fig. 1, the failure of the core induces a collapse of the tunnel, and the advance core is directly related to the tunnel stability. However, the length of the advance core was not clearly defined in this concept. In particular, although the length is primarily related to the geo-mechanical behavior of the ground, the length can be influenced by the seepage force at the tunnel face.

Based on the advance core concept, a computational model is modeled to estimate the face stability as influenced by the hydro-

*Member, Postdoctoral Fellow, Geotechnical Engineering Division, KIGAM, Daejeon 305-350, Korea. (E-mail:esoohong@yahoo.co.kr)
**Senior Researcher, Geotechnical Engineering Division, KIGAM, Daejeon 305-350, Korea. (Corresponding Author, E-mail: espark@kigam.re.kr)
***Principal Researcher, Geotechnical Engineering Division, KIGAM, Daejeon 305-350, Korea. (E-mail: shinhs@kigam.re.kr)
****Senior Researcher, Geotechnical Engineering Division, KIGAM, Daejeon 305-350, Korea. (E-mail: kimh@kigam.re.kr)

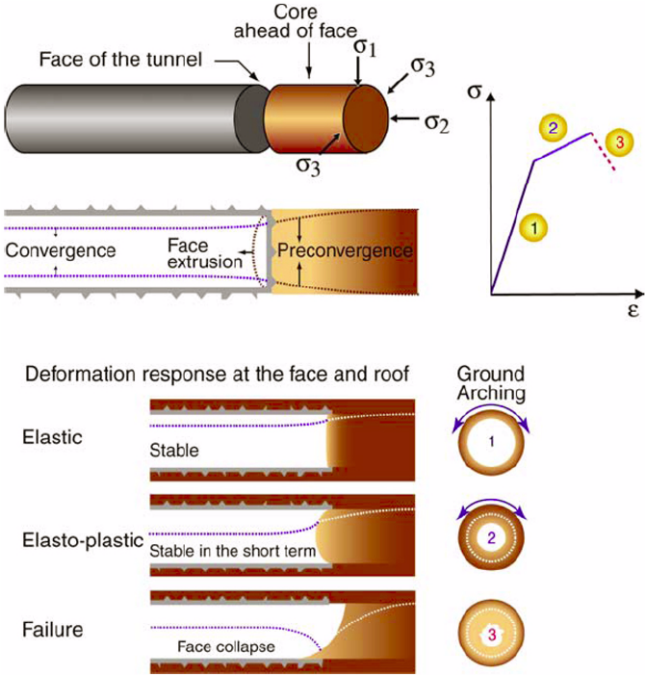

Fig. 1. Lunardi's Advance Core Concept (Jeon *et al.*, 2005)

logical characteristics of the ground. Three-dimensional steady-state seepage analyses are performed to evaluate parameters related to the model. Finally, the hydrological effects of a hazardous zone which shows high hydraulic conductivity and high water pressure on the stability of the tunnel face are analyzed.

2. Computational Model of the Seepage Force

The seepage force acting on the tunnel face can be modeled on the basis of the advance core concept, as shown in Fig. 2. As an advance core, a hypothetical cylinder has the cylindrical shape volume of the ground. The longitudinal boundary limit of the hypothetical cylinder is defined by the seepage force. In this model, the following assumptions are made:

1. The ground is homogeneous and is an isotropic material; additionally, it has no tension strength.
2. The hydraulic conductivity of the ground has identical values in all directions, and the direction of the seepage force is parallel to the tunnel axis.
3. The failure shape of the ground is cylindrical, and the Mohr-Coulomb failure criterion is realistic.
4. The hypothetical cylinder is a rigid body, and the body force by gravity is ignored.
5. The hazardous zone ahead of the tunnel face lies perpendicular to the tunnel axis.
6. The tunnel is circular with atmospheric pressure acting inside of it.
7. Deformation pertaining to the ground and the tunnel is disregarded.

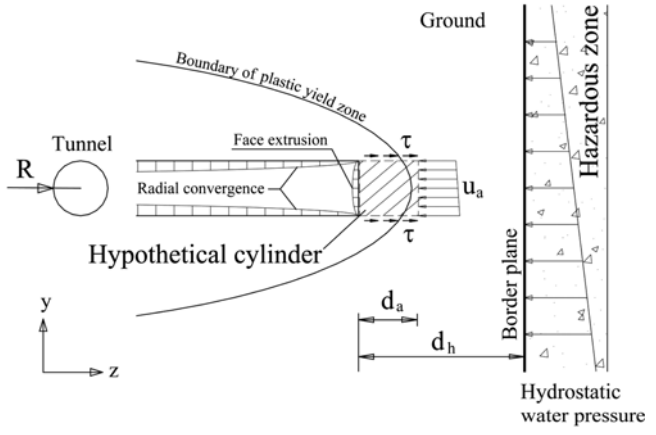

Fig. 2. Extrusion of the Tunnel Face Induced by the Failure of the Advance Core (Hoek, 2001), and the Concept of the Computational Model Utilized in this Study

As shown in Fig. 2, the radius of the tunnel is R, the distance from the tunnel face to an arbitrary position is d_a, and the distance between the tunnel face and the hazardous zone is d_h. Pore water pressure acting on a circular surface of the hypothetical cylinder is denoted as u_a. The combined force of the pore water pressure (i.e., the seepage force) mobilizes the unit skin friction τ on the surface of the circumference of the hypothetical cylinder. The driving force S as the seepage force is induced by the pore water pressure is as follows:

$$S = u_a(\pi R^2) \tag{1}$$

The maximum resisting force by the ground around the hypothetical cylinder T is

$$T = \tau(2\pi R d_a) \tag{2}$$

where the unit skin friction τ is given by

$$\tau = C + (\sigma - u_a)\tan\Phi \tag{3}$$

The cohesion C and the friction angle Φ denote the drained strength parameter of the ground, and s represents the average normal stress of the ground.

The ratio of the resisting force (T) to the driving force (S), TSR, is,

$$TSR = T/S = 2\frac{d_a}{R}\left(\frac{C + (\sigma - u_a)\tan\Phi}{u_a}\right) \tag{4}$$

Eq. (4) shows that the face stability of a deep tunnel is a function of the confinement, water pressure, strength parameters, advance core length (d_a), and tunnel size. In the area around the tunnel face, the behavior of the ground is complicated as a consequence of stress re-distribution after excavation. Considering that the TSR is related to only the seepage force, the TSR is not a true safety factor.

3. Analysis Model and Procedure

3.1 Model Boundary and Geometry of the Tunnel

A model boundary of a sufficient size is very important in a

seepage analysis to avoid adverse influence on the analysis results. The model boundaries are located at the flowing ranges to avoid a boundary effect. The dimensions here are as follows: (1) the horizontal range of the model is 50 times the radius of the tunnel; (2) the longitudinal range is approximately 70 times the tunnel radius; (3) the bottom range is approximately 18 times the tunnel radius. The boundary ranges and conditions are shown in Fig. 3.

It is assumed that the rock cover of the subsea tunnel is 100 m and that the depth of the seawater is 60 m, which is the average depth of the seawater in the southern part of the Korean Peninsula. The radii of the tunnels are 0.75, 1.5 m, 3 m, and 5.8 m.

3.2 Boundary Condition

In Fig. 3, the water table is fixed due to the infinite inflow of seawater. The total head (pressure head + elevation head = 271.6 m) at the top of the seawater is fixed throughout the analysis. The bottom and left (the opposite side of the vertical plane of symmetry of the ground) surfaces of the ground were also modeled as constant and identical to the total head (271.6 m). In addition, the vertical symmetry plane through the tunnel axis is prescribed as a no-flow boundary. For the condition of a permeable shotcrete lining on the ground surface, a zero pore water pressure was prescribed along the shotcrete-opened space (air) boundary, and flow into the tunnel was permitted.

3.3 The Hazardous Zone

The relative soil-lining stiffness, relative soil-lining hydraulic conductivity, and geometric factors (the ground water level, distance to an impervious layer, and location of water sources) are the major factors affecting tunnel lining loads (Bilfinger, 2005). Under the same concept, the relative hydraulic conductivity of the hazardous-ground zone (k_h/k_g; simply the relative hydraulic conductivity in this paper) and the distance between the tunnel face and the hazardous zone (d_h) are assumed as the major factors affecting the seepage force.

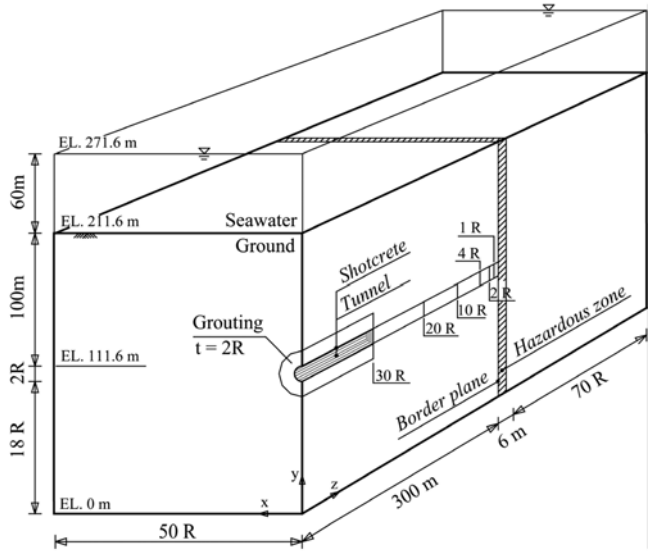

Fig. 3. Three-dimensional Analysis Condition

The hydraulic conductivity of a fault gouge is very small (Sausgruber and Brandner, 2003; Uehara and Shimamoto, 2006) and is similar to the hydraulic conductivity of clay (10^{-6} cm/sec order). However, fault breccia consists of cohesionless materials with high Young's moduli and high compressive strength values; moreover, it shows high hydraulic conductivity (Sausgruber and Brandner, 2003) similar to sand or gravel (more than 10^{-3} cm/sec order). To simplify the analysis case, it was assumed that the hazardous zone is vertically located on the ground with a width of 6 m.

3.4 Grouting Zone

Basically, the lining structure of a tunnel cannot support 1.6 MPa (a pressure head of 160 m) of water pressure. Hence, a tunnel should have a drainage system to reduce the water pressure. However, amount of inflow water due to high water pressure should be controlled in order to keep maintenance costs low. Grouting is a useful method to control the inflow water and improve the mechanical properties of the ground around the tunnel. In this study, only the hydraulic characteristic of the grouting zone is considered. It was assumed that the extent of grouting is 2 R from the tunnel surface.

3.5 Material Properties

The ground is assumed to be a homogeneous medium. The material properties and other relevant parameters are shown in Table 1.

3.6 Analysis Procedure

Continuous excavation of a tunnel with an intermediate to relatively low advance rate (for example, <500 m/month) and relatively high ground hydraulic conductivity (for example, $>10^{-4}$ cm/sec) will give a steady-state flow condition (Anagnostou, 2005). Three-dimensional steady-state seepage analyses were conducted with the commercial code MIDAS GTS® (Ver. 2.1). The numerical analyses were conducted based on the following procedure: 1) A total of 16 seepage analyses were conducted with four different tunnel radii (R = 0.75, 1.5, 3, and 5.8 m) and four different hazardous zone hydraulic conductivity values (1.0×10^{-7}, 1.0×10^{-6}, 1.0×10^{-5}, and 1.0×10^{-4} cm/sec, i.e., the relative hydraulic conductivity k_h/k_g in these cases is 1, 10, 100, and 1000, respectively); 2) each analysis case consists of six steps during the excavation stage (d_h = 30 R, 20 R, 10 R, 4 R, 2 R, and 1 R); 3) from the analyses result, pore pressure values that

Table 1. Material Properties

	Ground	Grouting	Hazardous zone	Shotcrete
k (cm/sec)	1.0×10^{-7}	1.0×10^{-10}	1.0×10^{-4} - 1.0×10^{-7}	1.0×10^{-7}
C (kPa)	700	900	70	-
Φ (×)	40	40	40	-
γ(kN/m^3)	23	24	23	25
thickness	-	1D	6 m	25 cm

depend on the magnitude of d_a (0, 1 R, 2 R, 3 R, 4 R, 6 R, and 8 R) are acquired in each analysis case and excavation stage; 4) finally, the hydraulic gradients i and the ratios of the driving force and the resisting force TSR are estimated.

4. Analysis Results and Discussions

4.1 Effects of the Hazardous Zone on the Pore Water Pressure Distribution

In conditions that include homogeneous saturated ground (i.e., no hazardous zone) and a constant rate of advance, the distribution of the pore water pressure 'u_a' at the arbitrary point ahead of the tunnel is independent of the location of the tunnel face (i.e., the excavation stage). However, if the ground has a hazardous zone ahead of the tunnel face, in every location of the tunnel face the distribution of u will show different trends. Fig. 4 is a typical analysis result of the pore pressure distribution. Fig. 4 shows the re-distributed pore water in the ground influenced by the tunnelling and a hazardous zone.

Fig. 5(a) (step 2) can be considered as a result representing absence of a hazardous zone. However, as shown in Figs. 5(b) and (c), the hazardous zone produces a gradual change of the hydraulic gradient distribution with a decrease in the distance between the tunnel face and the hazardous zone, d_h. In Figs. 5(b) and (c) (Steps 3 and 4), a contour line in which the hydraulic gradient reaches 1.0 is more enlarged in the upper and lower sides compared to Step 2. In addition, the hydraulic gradient of the inner domain of the hazardous zone shows nearly a zero value.

Similar to what is shown in Fig. 5, the hydraulic gradient in the

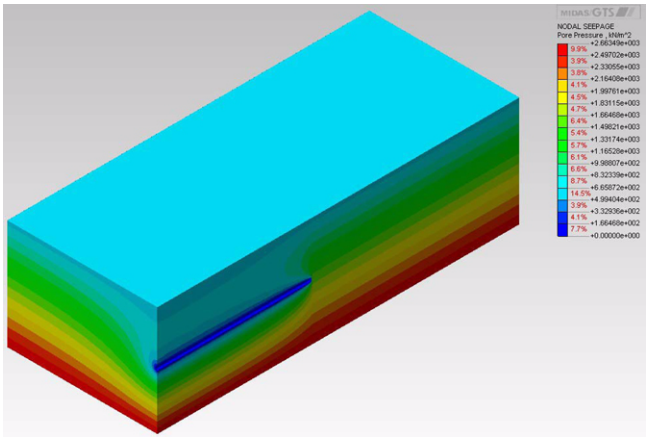

Fig. 4. 3-Dimensional Pore Pressure Distribution (k_h/k_g = 1000, R = 3 m, d_h = 2 R)

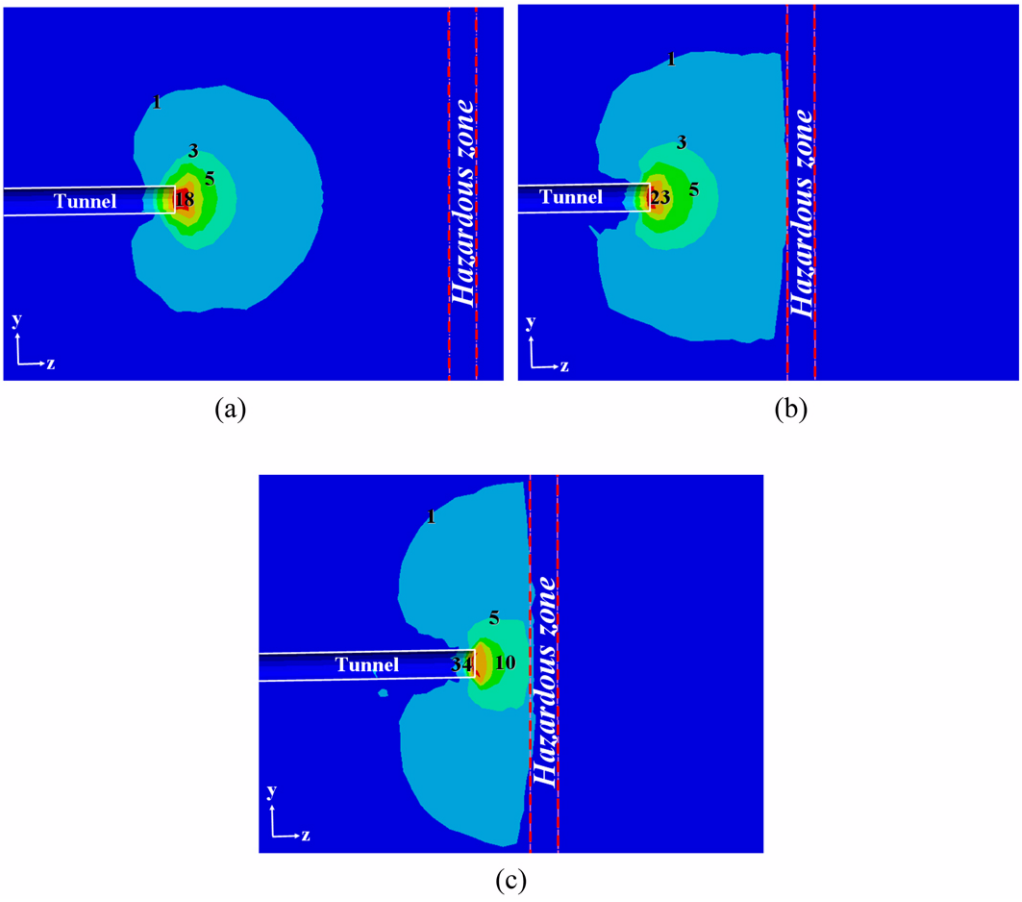

Fig. 5. Effect of the Hazardous Zone on the Distribution of the Hydraulic Gradient in the z-Direction with the Tunnel Advance (R = 3 m, k_h/k_g = 1000): (a) Step 2 (d_h = 20 R), (b) Step 3 (d_h = 10 R), (c) Step 4 (d_h = 4 R)

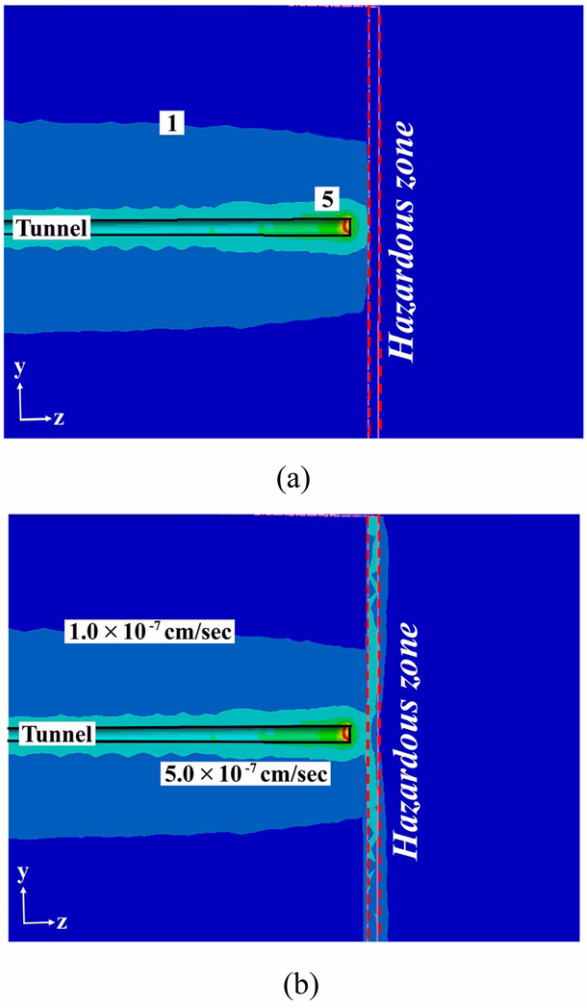

Fig. 6. Effect of the Hazardous Zone on the Distribution of the Hydraulic Gradient and the Flow Water Velocity in the xyz-Direction (R = 3 m, k_h/k_g = 1000): (a) The Hydraulic Gradient, (b) The Water Flow Velocity

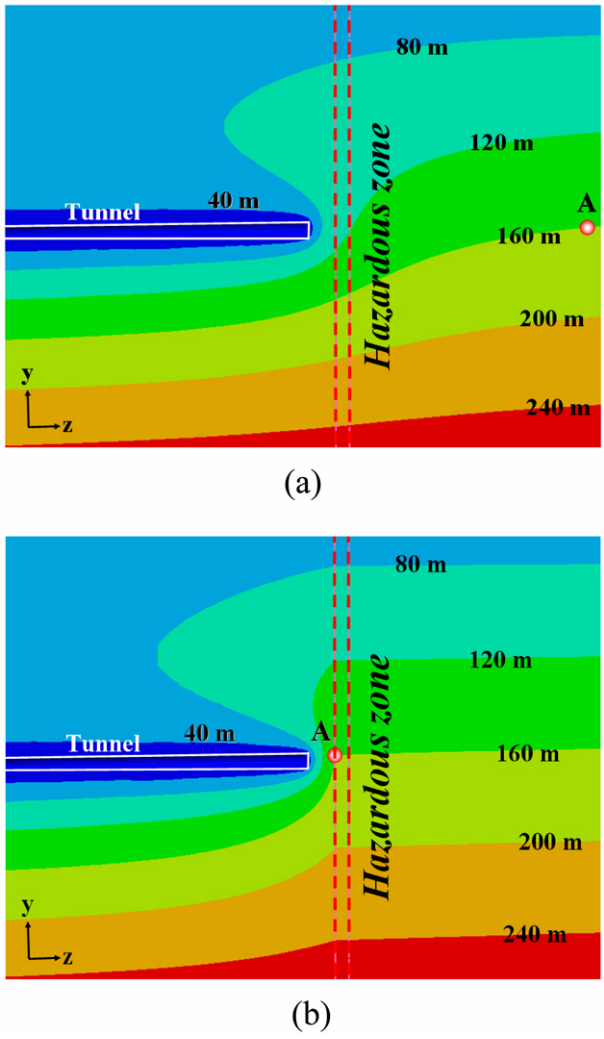

Fig. 7. Variation of the Pore Water Pressure due to the Relative Permeability of the Hazardous-ground Zone, k_h/k_g (R = 3 m, d_h = 4 R): (a) k_h/k_g = 1, (b) k_h/k_g = 1000

xyz-direction shows nearly a zero value in the hazardous zone (Fig. 6(a)). The water flow velocity at the boundary of the hazardous zone is nearly identical to the velocity at which the hydraulic gradient is 1.0 (1.0×10^{-7} cm/sec), as shown in Fig. 6(a). However, the velocity increases more in the hazardous zone and is nearly identical to the velocity at which the hydraulic gradient is 5.0 (5.0×10^{-7} cm/sec). This is caused by the incoming and moving speed of the ground water in the hazardous zone, which is faster than the outgoing speed through the excavated tunnel face. The hazardous zone represents the major route for the infinite inflow of water due to its hydraulic conductivity.

The distribution of the pore water pressure depends on the magnitude of the relative hydraulic conductivity. Under ordinary conditions (k_h/k_g = 1), approximately 160 m of the far-field hydrostatic pore pressure head at the ceiling level (EL. 111.6 m in Fig. 6) of the tunnel acts on point (A), which is located far from the tunnel face (Fig. 7(a)). This result is similar to other research results (Anagnostou and Kovari, 1996; Pellet *et al.*, 1993). However, when the relative hydraulic conductivity value reaches 1000, the far-field hydrostatic pore pressure is generated at the border plane (Fig. 7(b)).

If the relative hydraulic conductivity is less than 1000, this trend depends on the tunnel size and d_h (Fig. 8). In Fig. 8, the 'pressure head ratio' is the ratio of the water head reduced by excavation to the hydrostatic pressure at an arbitrary point on the border plane at the tunnel ceiling level. When the relative hydraulic conductivity value is greater than 50 and the d_h value is greater than 5 R, approximately 90% of the far-field hydrostatic pore water pressure acts on the border plane. Bilfinger (2005) reported that when the value of the relative ground-lining hydraulic conductivity (k_{ground}/k_{lining}) is higher than 50, the induced pressure value of the lining will be nearly equal to the far-field hydrostatic pore pressure value. In the same manner, the stability of the ground ahead of the tunnel face will be affected significantly by the values of the relative hydraulic conductivity.

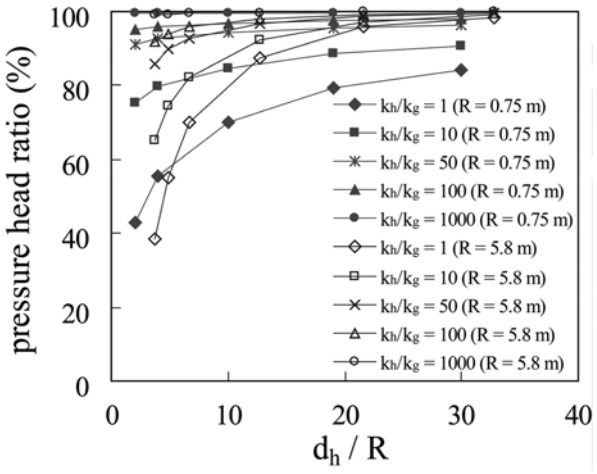

Fig. 8. Distribution of the Pressure Head Ratio at the Border Plane

4.2 Effects of the Seepage Force Induced by a Hazardous Zone on the Stability of the Tunnel Face

The distribution of the hydraulic gradient and the TSR in the ground ahead of the tunnel face can be a significant index to estimate the distribution of the seepage force and the manner in which the face stability is affected by the seepage force.

To explore the effect of a hazardous zone on the distribution of the seepage force and the stability of the tunnel face, the hydraulic gradient and the TSR are plotted versus d_a/R in Fig. 9.

The hydraulic gradient values increase as the d_a/R values decrease (Fig. 9(a)), and the TSR values increase (Fig. 9(b)). The hydraulic gradient values increase as the radius of the tunnel decreases. However, the TSR values are nearly independent of the d_a/R values. In Fig. 9(b), the TSR values show little difference with respect to the R values. The area of the tunnel face as a drainage surface is proportional to the square of the radius of the tunnel. The amount of the inflow water and the range of influence of the drainage effect both increase with the area of the tunnel face. The distances between the equipotential lines of the hydraulic gradient for the small radius of a tunnel in the vicinity of the tunnel face are relatively short. As a result, in the vicinity of the tunnel face, the hydraulic gradient values and the pore water pressure values of the large radius of a tunnel are smaller than those of a small radius of a tunnel. However, the magnitude of the seepage force also increases with the area of the tunnel face; thus, the magnitude of the TSR values is nearly independent of the radius of the tunnel.

As shown in Figs. 9(a) and (b), when the values of d_a exceed approximately five times those of R, the values of the hydraulic gradient decrease and the TSR increases rapidly. In addition, the TSR value is more dependent on the ground condition and d_a/R (Fig. 10) than it is on the radius of the tunnel (Fig. 9(b)). As shown in Fig. 10, the TSR value becomes 1 when d_a/R is 1 and when the ground condition is poor ($C = 200$ kPa, $\Phi = 20^o$). High water pressure can induce a failure of the ground at the tunnel face by itself in conjunction with a poor ground condition.

The effects of a hazardous zone on the distribution of the seepage force and stability of the tunnel face can be easily identified through comparisons with 'no hazardous zone' cases. With i_o representing the hydraulic gradient of the 'no hazardous zone'

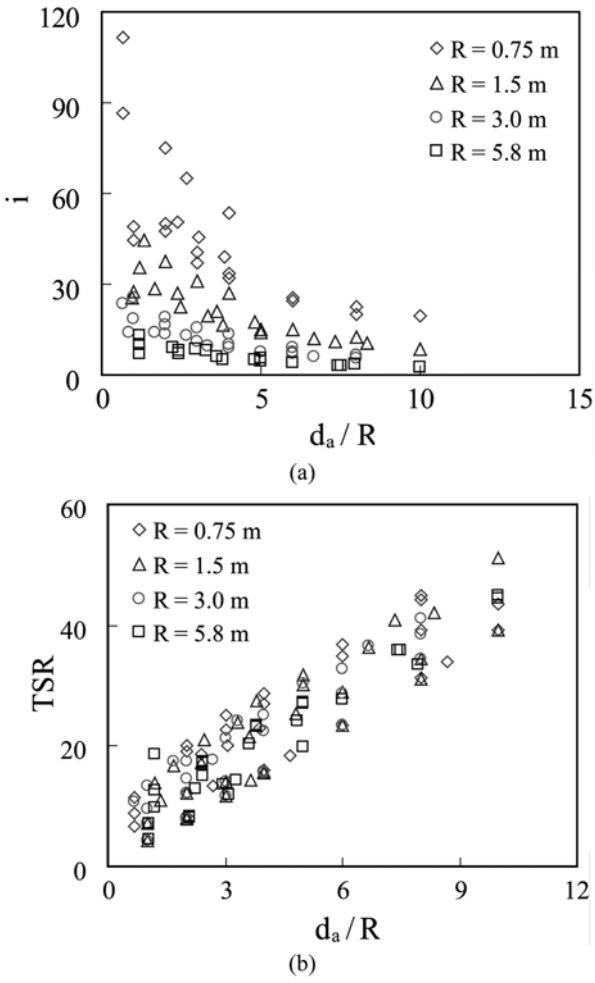

Fig. 9. Distribution of the Hydraulic Gradient i and the Ratio of Driving Force to Resisting Force with Respect to d_a/R (at k_h/k_g = 1000): (a) i vs d_a/R, (b) TSR vs d_a/R

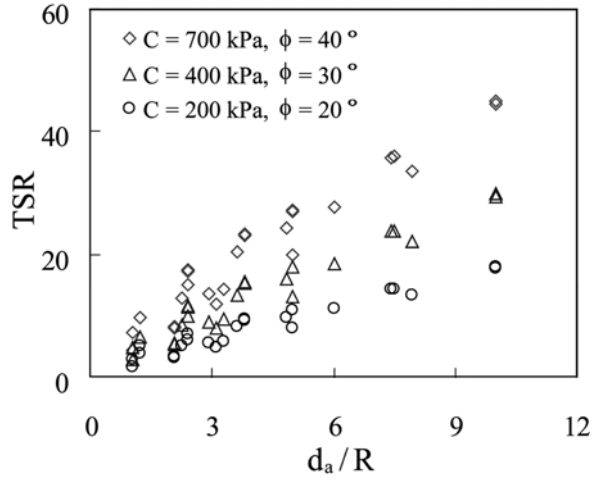

Fig. 10. Effect of the Strength Parameters to the TSR (at k_h/k_g = 1000; R = 5.8 m)

and TSR_o representing the TSR value of the 'no hazardous zone,' the effect of the hazardous zone on the tunnel face was analyzed with the i/i_o ratio and the TSR/TSR_o values of each excavation stage. Although Figs. 11 and 12 show the results when d_a is equal to 0.5, these figures show a typical trend. In Figs. 11 and 12, the i/i_o ratio and/or the TSR/TSR_o values are nearly 1.0 when the

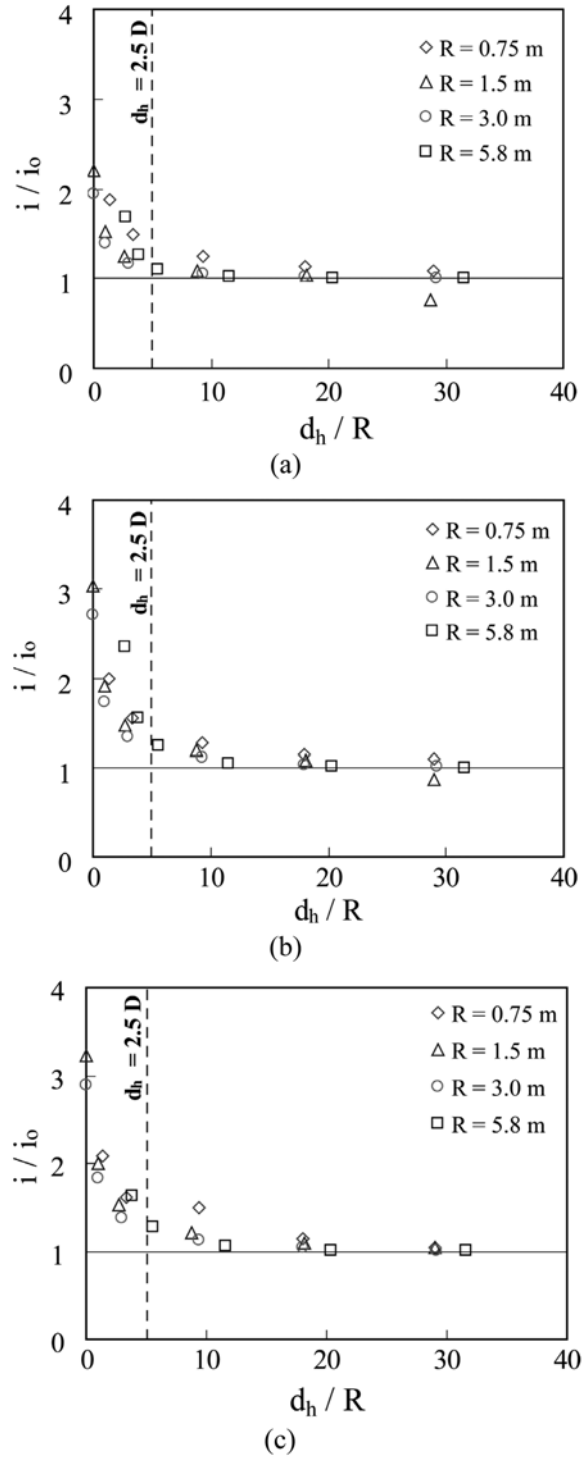

Fig. 11. Distribution of the Normalized Hydraulic Gradient i/i_o with the Normalized Distance between the Tunnel Face and the Hazardous Zone d_h/R (at $d_a = 1$ R): (a) i/i_o vs d_h/R at $k_h/k_g = 10$, (b) i/i_o vs d_h/R at $k_h/k_g = 100$, (c) i/i_o vs d_h/R at $k_h/k_g = 1000$

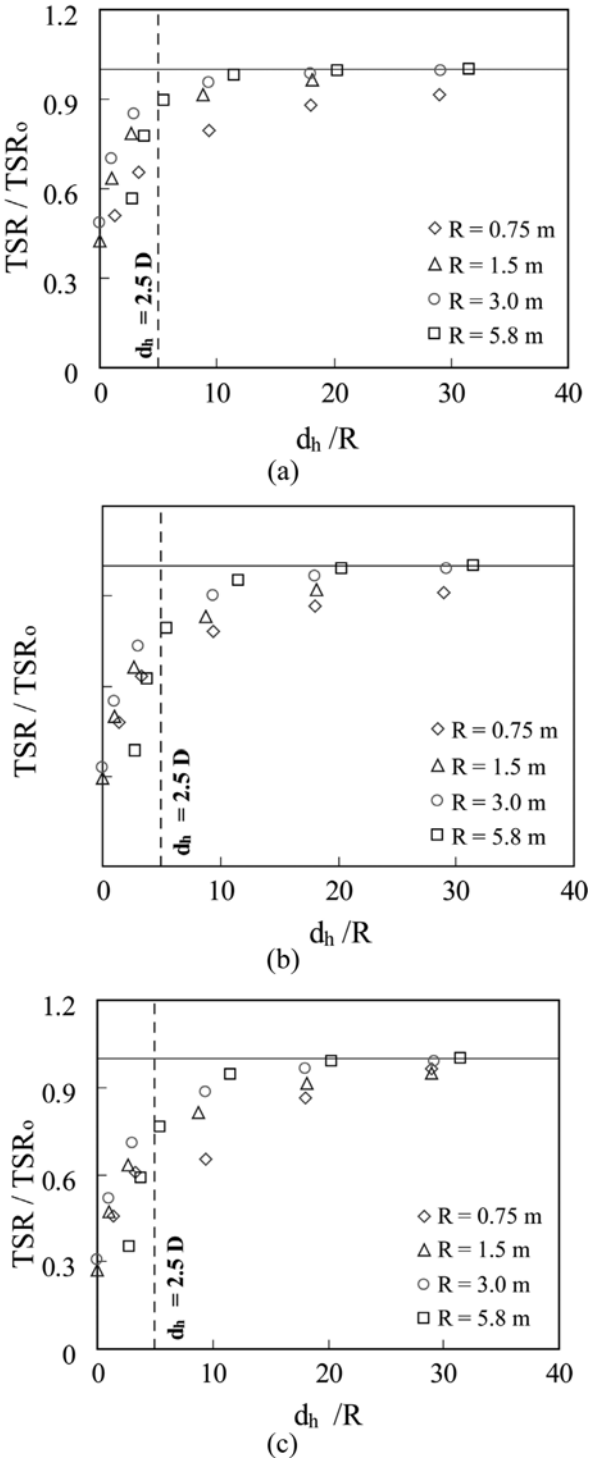

Fig. 12. Distribution of the Normalized Driving Force to Resisting Force Ratio TSR/TSR_o with the Normalized Distance between the Tunnel Face and the Hazardous Zone d_h/R (at $d_a = 1$ R): (a) TSR/TSR_o vs d_h/R at $k_h/k_g = 10$, (b) TSR/TSR_o vs d_h/R at $k_h/k_g = 100$, (c) TSR/TSR_o vs d_h/R at $k_h/k_g = 1000$

tunnel face is located far enough away from a hazardous zone. Changes start when the d_h/R value is close to 10~20. When the d_h values are in the range of 0 to 5 times the value of R, the values of i/i_o rapidly increase and the values of TSR/TSR$_o$ rapidly decrease. These trends are independent of the size of the tunnel (R) and the relative hydraulic conductivity. The estimated length of the advance core depending only on the mechanical characteristics of the ground is 4 to 6 times the value of R (Lunardi, 2000). In a homogeneous ground condition, when a weak zone is placed 1.0 R ahead of the tunnel face, the vertical displacement of the tunnel face changes rapidly (Jeon *et al*., 2005; Baek *et al*., 2006). Therefore, the influence range of the hydrological characteristics of the hazardous zone on the stability of the face is greater than that of the mechanical characteristics.

The hydrological characteristics of a hazardous zone can have additional effects on the face stability of a tunnel when stability is poor due to mechanical characteristics. Face failure in the vicinity of a hazardous zone can induce many risks, such as flooding accidents. To reduce these risks, systematic probe-drilling can be a good countermeasure. The drilling range should be more than five times the radius of the excavated tunnel.

5. Conclusions

In this study, the effects of high water pressure in a localized high hydraulic conductivity zone (hazardous zone) on the stability of a tunnel face were analyzed. This study is not a fully coupled hydro-mechanical analysis but a hydrological analysis. Therefore, these results cannot reflect the true site conditions, and the TSR is not a true safety factor. However, the TSR is a simple and effective indicator for analyzing the stability of a tunnel that is affected by a hazardous zone. The results of this study clearly reflect the hydrological effect of the hazardous zone. Three-dimensional steady-state seepage analyses led to the following results:

- The magnitude of the relative hydraulic conductivity value directly influences on the distribution of the hydraulic gradient and the pore water pressure. When the relative hydraulic conductivity value is greater than 50 and the d_h value is greater than 5 R, approximately 90% of the far-field hydrostatic pore water pressure is generated at the border plane. Therefore, the hydrostatic pore water pressure acts on most of the hazardous zones throughout all of the tunneling stages.
- The maximum influence range of the hydrological characteristics of the hazardous zone on the face stability is within 20 times the R value. When the d_h value is approximately five times the R value, the influence increases rapidly. These influence ranges are greater than that of the mechanical characteristics.
- The TSR value depends more on the ground condition and on d_a/R than it does the radius of the tunnel. When d_a/R is 1 in conjunction with a poor ground condition (C = 200 kPa, Φ = 20°), TSR becomes 1.
- When the stability is poor due to the mechanical characteristics, a hazardous zone aggravates the stability of the face of a subsea tunnel. Consequently, face failure in the vicinity of a hazardous zone can induce flooding accidents.

Acknowledgements

This study was funded by the Korea Institute of Construction & Transportation Technology Evaluation and Planning under the Ministry of Construction & Transportation in Korea (Grant No. 05-D10, Development of Water Control Technology in Undersea Structures).

References

Anagnostou, G. (2005). "The influence of tunnel excavation on the hydraulic head." *International Journal of Analytical Methods in Geomechanics*, Vol. 19, No. 10, pp. 725-746.

Anagnostou, G. and Kovari, K. (1996). "Face stability conditions with earth-pressure-balanced shields." *Tunneling and Underground Space Technology*, Vol. 11, No. 2, pp. 165-173.

Arjnoi, P., Jeong, J. H., Kim, C.Y., and Park, K. H. (2009). "Effect of drainage conditions on porewater pressure distributions and lining stresses in drained tunnels." *Tunneling and Underground Space Technology*, Vol. 24, No. 4, pp. 376-389.

Baek, S. H., Kim, C. Y., Kim, K. Y., Hong, S. W., and Moon, H. K. (2006). "Numerical analysis on the effect of heterogeneous nature of rock masses on tunnel behavior." *Tunneling Technology*, Vol. 8, No. 2, pp. 115-127.

Bilfinger, W. (2005). "Design procedures for ground water loads on tunnel linings." http://www.ita-aites.org/cms/ita-aites-home/publications/conferences-proceedings/conferences-proceeding-detail/datum/2008/07/06/sao-paulo-2005-waterproofing.html.

Bobet, A. (2001). "Analytical solutions for shallow tunnels in saturated ground." *J. Eng. Mech.*, ASCE., Vol. 127, No. 2, pp. 1258-1266.

Buergi, C., Parriaux, A., Franciosi, G., and Rey, J-Ph. (1999). "Cataclastic rocks in underground structures - Terminology and impact on the feasibility of projects (Initial results)." *Engineering Geology*, Vol. 51, No. 3, pp. 225-235.

El Tani, M. (2003). "Circular tunnel in a semi-infinite aquifer." *Tunneling and Underground Space Technology*, Vol. 18, No. 1, pp. 49-55.

Hoek, E. (2001). "The thirty-sixth Karl Terzaghi lecture: Big tunnels in bad rock." *J. Geotech. Geoenviron. Eng.*, ASCE., Vol. 127, No. 9, pp. 726-740.

Hong, E. S., Shin, H. S., Park, C., Kim, H.M ., and Park, E. S. (2007). "Numerical study on horizontal pre-drainage system using horizontal directional direction drilling in subsea tunneling." *Chinese J. of Rock Mech. and Eng*., Vol. 26, No. Supp. 2, pp. 3697-3703.

Jeon, J. S., Martin, C. D., Chan, D. H., and Kim, J. S. (2005). "Predicting ground conditions ahead of the tunnel face by vector orientation analysis." *Tunneling and Underground Space Technology*, Vol. 20, No. 4, pp. 344-355.

Kong, J. S., Choi, J. W., Nam, S. W., and Lee, I. M. (2006). "Tunnel-lining analysis in consideration of seepage and rock mass behavior." *Journal of the Korean Society of Civil Engineers*, Vol. 26, No. 5C, pp. 359-368. (in Korean)

Leca, E. and Dormieux, L. (1990). "Upper and lower bound solutions for the face stability of shallow circular tunnels in frictional material." *Geotechnique*, Vol. 40, No. 4, pp. 581-606.

Leca, E. and Panet, M. (1988). "Application du calcul à la rupture à la stabilité du front de Taille Dùn tunnel." *Revue Francaise de*

Geotechnique, Vol. 43, pp. 5-19.

Lee, I. M. and Nam, S. W. (2001). "The study of seepage forces acting on the tunnel lining and tunnel face in shallow tunnels." *Tunneling and Underground Space Technology*, Vol. 16, No. 1, pp. 31-40.

Lunardi, P. (2000). "Design and construction of tunnels using the approach based on the analysis of controlled deformation in rocks and soils." *Tunnels Tunn. Int*., Special Suppl., pp. 3-30.

Park, K. H., Lee, J. G., Owatsiriwong, A. (2008). "Seepage force in a drained circular tunnel: An analytical approach." *Can. Geotech. J.*, Vol. 45, No. 3, pp. 432-436.

Pellet, F., Descoeudres, F., and Egger, P. (1993). "The effect of water seepage forces on the face stability of an experimental microtunnel." *Can. Geotech. J.*, Vol. 30, No. 2, pp. 363-369.

Sausgruber, T. and Bradner, R. (2003). "The relevance of brittle fault zones in tunnel construction - Lower inn valley feeder line north of Brenner Base tunnel, Tyrol, Austria." *Mitt. Osterr. Geol. Ges*., Vol. 94, pp. 157-172.

Schubert, W. and Steindorfer, A. (1998). "Effect of seepage forces on the shotcrete lining of a large undersea cavern." *Proceedings, Int. Conf. Computer Methods and Advances in Geomechanics*, Rotterdam, pp. 1205-1208.

Schweiger, H. F., Pottler, R. K., and Steiner, H. (1991). *Effect of seepage forces on the shotcrete lining of a large undersea cavern*, Computer Method and Advances in Geomechanics, Rotterdam, pp. 1503-1508.

Uehara, S. and Shimamoto, T. (2006). "Estimation of permeability structure of the median tectonic line fault zone in Ohshika-Mura, Nagano, Japan, by using laboratory test under high pressure." *4th Asian Rock Mechanics Symposium*, Singapore, p. 314.

Wise, D. U., Dunn, D. E., Engelder, J. T., Geiser, R. A., Hatcher, R. D., Kish, S. A., Odom, A. L., and Schamel, S. (1984). "Fault-related rocks: Suggestions for terminology." *Geology*, Vol. 12, No. 7, pp. 391-394.